EARTHQUAKE DAMAGE DETECTION USING EOS/ASTER MULTI-TEMPORAL IMAGES BASED ON IMAGE FLUCTUATION MODEL METHOD

Masayuki KOHIYAMA[1] and Fumio YAMAZAKI[2]

ABSTRACT: A new damage or change detection method using middle-resolution satellite images is proposed, which employs the probability distribution model of the digital number (DN) fluctuation in a normal condition and its significance test. The DN fluctuation model is formulated by considering imaging process of a satellite sensor and image registration process. A result thematic map is created from significance levels which are defined on a pixel basis as follows: the minimum significance level with which a null hypothesis that the pixel DN can be considered as a sample of the DN fluctuation model is rejected. The proposed method overcomes the threshold setting problem in conventional change detection methods. The method is applied to the 2001 Bhuj, India earthquake and the 2003 Bam, Iran earthquake. Though the detected possible damaged areas are narrower than the actual damaged areas, the relatively similar results were obtained compared with the visual inspection results of high resolution satellite images.

Key Words: Remote sensing, damage detection, 2001 Bhuj, India earthquake, 2003 Bam, Iran earthquake, EOS/ASTER, multi-temporal images

INTRODUCTION

Although high-resolution satellite imagery gathers people's attention with its imaging capability, middle-resolution satellite imagery (e.g. Landsat-TM, Landsat-ETM+, SPOT-HRV, and EOS/ASTER), of which ground sampling interval is larger than 10m, could be utilized for damage detection. This is because of the following reasons: 1) its wider swath can depict the perspective view of wide-ranging disaster areas, 2) its ample archive of previously acquired images can provide a pre-event image of almost any place after a disaster reliably. In addition, the cost of the image per area is considerably lower than that of high-resolution one. It is the commonly accepted that all the available information should serve for disaster relief activities, and thus, we have to promote researches to devise damage detection methods using middle-resolution imagery as well as higher-resolution one.

This paper proposes a new damage (change) detection method by introducing a probability model of digital number (DN) fluctuation in an image pixel and its significance test. The method overcomes the uncertainty, arbitrariness and difficulty of threshold setting in conventional change detection methods. This is the generalized method from the method originally provided by Kohiyama et al. (2004) based on DMSP/OLS nighttime images.

[1] Research Associate
[2] Professor, Department of Urban Environment Systems, Faculty of Engineering, Chiba University

THRESHOLD SETTING PROBLEM IN DAMAGE (CHANGE) DETECTION

Determining a threshold value to discriminate damage and no damage, or change and no change is a difficult task. Many researchers have proposed change detection procedures: comparison of land cover classifications, multi-date classification, image differencing/ratioing, index differencing (e.g. vegetation index, tasseled-cap indices), principal components analysis, and change vector analysis (Singh, 1989). But, in the final stage of most techniques, change and no change may be judged by a simple thresholding as a '0-1' binary response:

$$change(x,y) = \begin{cases} 0 & (f(\mathbf{DN}) \le T) \\ 1 & (f(\mathbf{DN}) > T) \end{cases} \tag{1}$$

where x and y mean the target location on the ground, the vector **DN** means DNs of satellite images (can also mean multi-band and/or multi-temporal data), and T is the threshold value supplied empirically or statistically by the analyst. Once you introduce threshold values, you can evaluate the change in categorical attributes of the target areas, e.g. from forest to urban, from no change to change, etc. But, in case of damage detection, we often face the lack of reference data of damage areas and a threshold value derived from few reference data is unreliable; moreover, a threshold value may change from region to region, and country to country because urban structures have such variety that a certain threshold may not be valid for a different city any longer.

Morisette et al. (1999) proposed to use generalized linear models (GLMs) in change detection and to generate a thematic map of 'probability of (category) change'. Kohiyama et al. (2004) proposed to use significance levels in a thematic map. Probability expression can help us to avoid the uncertainty and arbitrariness of threshold values and has the great advantage that people easily understand the credibility of the evaluation result. However, GLMs such as logit and probit model require sample reference data in the regression analysis, and deficiency of reference images of earthquake damage and the above-mentioned regional differences hinder us to employ GLMs. Thus, a new approach is necessary to address these problems.

DIGITAL NUMBER AS A RANDOM VARIABLE

Our proposing method to detect damage is based on a principle that DN of a fixed point can be considered as a random variable, which changes and fluctuates even in a normal (non-disaster) situation. This section explains how DN can be modeled into a random variable based on the overall sensor model of an electro-optical remote-sensing system (Schowengerdt, 1997).

In scanning operation of a satellite sensor, the radiance of band b, s_b is converted into the electric signal, e_b:

$$e_b(x,y) = \iint s_b(\alpha,\beta)\, PSF(x-\alpha, y-\beta)\, d\alpha d\beta \tag{2}$$

where PSF is the point spread function (PSF) of the whole sensor system, and this includes optical process. As an example, the PSF of Landsat/TM is shown in Figure 1 (Schowengerdt, 1997). The A/D converter samples and quantizes the electric signal into discrete DN values, $P(x, y)$:

$$P(x,y) = \mathrm{int}(gain_b \times e_b(x,y) + offset_b) \tag{3}$$

where $gain_b$ and $offset_b$ represents the parameters of the linear A/D conversion.

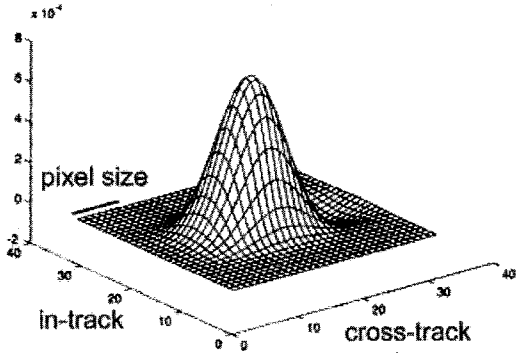

Figure 1. Point spread function of Landsat/TM (Schowengerdt, 1997; annotation is added by the authors).

These equations include conversion from continuous to discrete spatial coordinates implicitly. Usually, the discrete coordinates are different among images, and there exists a difference of the *sample-scene phase*, or pixel center offset, that is the relative location of the pixels and the target. The relative spatial phase is unpredictable and mostly unknown for any given image acquisitions, and we assume it follows the two-dimensional uniform probability distribution between $\pm 1/2$ pixel for both cross-track and in-track directions.

In analysis using multi-temporal images, all the images are registered and the offsets are adjusted to the single reference image. The cubic convolution is one of the most popular interpolation methods in this registration process:

$$Q(x,y) = \mathrm{int}\left(\begin{bmatrix}\mathrm{sinc}(1+t) & \mathrm{sinc}(t) & \mathrm{sinc}(1-t) & \mathrm{sinc}(2-t)\end{bmatrix}\begin{bmatrix}P_{11} & P_{12} & P_{13} & P_{14}\\ P_{21} & P_{22} & P_{23} & P_{24}\\ P_{31} & P_{32} & P_{33} & P_{34}\\ P_{41} & P_{42} & P_{43} & P_{44}\end{bmatrix}\begin{bmatrix}\mathrm{sinc}(1+s)\\ \mathrm{sinc}(s)\\ \mathrm{sinc}(1-s)\\ \mathrm{sinc}(2-s)\end{bmatrix}\right) \quad (4)$$

where the $Q(x, y)$ is the integer DN of the registered image, the vector (x, y) is the location in the adjusted coordinate system, P_{ij} represent DNs of the sixteen points surrounding the point (x, y) as shown in Figure 2, and $\mathrm{sinc}(x) = \sin(\pi x) / (\pi x)$. The vector (s, t) represents the phase of two directions with each element raging from 0 to 1 (Figure 2), and this is a random variable following the 2-D uniform probability distribution, as we assumed. Therefore, by assuming there is no quantization in Equation (3), the DN of the registered image, $Q(x, y)$, is:

$$Q(x,y) \approx \mathrm{int}\left(gain_b \iint s_b(\alpha,\beta)\, SPSF(x-\alpha, y-\beta)\, d\alpha d\beta + offset_b\right) \quad (5a)$$

$$SPSF(x,y) = \sum_{i=1}^{4}\sum_{j=1}^{4} W_{ij}\, PSF(x-x_{ij}, y-y_{ij}) \quad (5b)$$

and

$$[W_{ij}] = \begin{bmatrix}\mathrm{sinc}(1+t)\\ \mathrm{sinc}(t)\\ \mathrm{sinc}(1-t)\\ \mathrm{sinc}(2-t)\end{bmatrix}\begin{bmatrix}\mathrm{sinc}(1+s) & \mathrm{sinc}(s) & \mathrm{sinc}(1-s) & \mathrm{sinc}(2-s)\end{bmatrix} \quad (5c)$$

where the vectors (x_{ij}, y_{ij}) represents the pixel center locations of the surrounding sixteen points. The Equation (5a), (5b) and (5c) describe the DN of a pixel is a random variable. Thus, the DN of the same target varies from acquisition to acquisition even in a normal, non-disaster condition.

Registration errors always remain even if sub-pixel accuracy is achieved in registration, and this increases the randomness of DNs. Obviously, there exist other well-known factors that increase the randomness: electronic noise in a sensor system, atmospheric correction errors, solar position difference (shade, shadow, etc.), phenological changes, soil moisture differences, relative ground sampling interval changing along the off-nadir scan angle, etc. The quantization error in Equation (3), which we assumed to be negligible in the formulation, is also one of the factors.

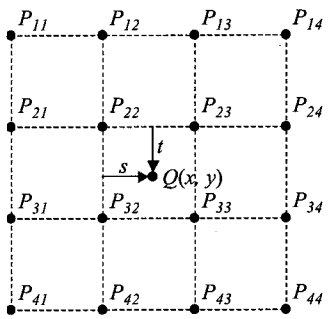

Figure 2. Registration by cubic convolution.

DAMAGE DETECTION METHOD BASED ON PROBABILITY MODEL OF DIGITAL NUMBERS IN MULTI-TEMPORAL IMAGES

Modeling of probability distribution of digital numbers

As formulated in the previous section, DN of each location can be modeled as a random variable. As the method to evaluate the probability distribution of DN, Equations (5a), (5b), and (5c) and the two-dimensional uniform distribution of the variables s and t can be employed. Or, multi-temporal images serve as sample data to evaluate the probability distribution. Although the number of the pre-event images may be limited, collecting these images is much easier than conventional approaches of change detections: gathering reference images of earthquake damage for training data and considering regional differences between the reference and target areas.

The DN fluctuation model for some categorized urban areas is an optional solution to increase the sample data, but it may result in decreasing change detection accuracy because pixels with different probability distributions are mixed up and the variance of the categorized model is clearly larger than that of a single pixel model.

Damage or change detection based on a significance test

If DN or fluctuation of DN is given as the probability distribution, $Pr(Q)$, where Q represents a DN in an image acquired in normal time, i.e. before a disaster. Now, we introduce the following null hypothesis:

Null hypothesis H_0: When the digital number, $q(x, y)$, of the location (x, y) on the ground is acquired, $q(x, y)$ is considered as a sample of the probability distribution, $Pr(Q)$.

and conduct a significance test based on a significance level of α. If q is in a range of small fluctuation and H_0 cannot be rejected, we have no other choice than taking that there is no change on the ground. But, if rejected, we can judge that there exists an abnormal change on the ground, which exceeds the fluctuation level in a normal time, i.e. possibly damage. Therefore, by conducting the significance test for each location, a significance level, $\alpha(x, y)$,which satisfies the following equation can be evaluated:

$$\int_{\mu-|q-\mu|}^{\mu+|q-\mu|} pr(Q)dQ = 1-\alpha \tag{6}$$

where $pr(Q)$ is a probability density function of $Pr(Q)$ and μ is the mean of the distribution (Figure 3). Note that $Pr(Q)$ can be any probability distribution other than normal distribution, but the mean μ must be given in advance in order to identify the significance level α from Equation (6).

As is mentioned, the DN fluctuation model for some categorized urban areas is an optional solution to increase the sample data, but it may result in decreasing change detection accuracy because pixels with different probability distribution are mixed up and the variance of the categorized model is clearly larger than that of a single pixel model.

Finally, the map of credibility (probability) of damage occurrence will be obtained by mapping the distribution of the risk percentage (significance level), $1-\alpha$.

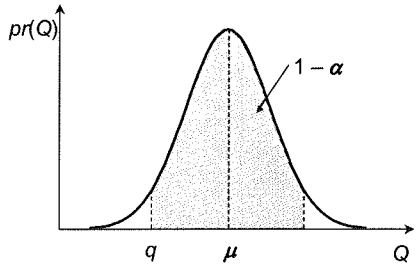

Figure 3. Evaluation of risk percentage (significance level), $1-\alpha$. In this example, q, which is a digital number acquired after a disaster, is smaller than μ.

Damage detection flow

Figure 4 shows the flow chart of our proposing method, the Image Fluctuation Model (IFM) method to detect damage (change) using middle-resolution satellite imagery:

Step 1: Collect the multi-temporal pre-event images
Step 2: Register these images and compensate atmospheric effects.
Step 3: Evaluate a probability distribution, $Pr(Q)$, for each DN using the above processed images.
Step 4: Acquire the post-event image.
Step 5: Process the post-event image for registration and atmospheric correction.
Step 6: Conduct the significance tests on a pixel basis for all the pixels in a target area using the probability models, $Pr(Q)$, by assuming the null hypothesis that DN is a sample of $Pr(Q)$ with the significance level α.
Step 7: Create a thematic map of $1-\alpha$ to depict the damage (change) probability of each pixel.

Any value of band data, index, or principal component can be the input variable, Q; and it is easy to expand the dimension of Q and $Pr(Q)$ into a higher order by using a multi-dimensional probability distribution. If the multi-dimensional Gaussian distribution is assumed as a DN fluctuation model, the contour surfaces of α become hyper-ellipsoid (Figure 5). This seems to be similar to the Ellipsoidal Change Detection (ECD) method proposed by Dai and Khorram (1998), which employs a Gaussian distribution and the Mahalanobis distance function of an n-dimensional difference image. But our IFM method substantially differs from ECD method; threshold setting is not required anymore while ECD method requires that. The resulting thematic map of IFM method shows the significance level of each pixel area, and it reflects the credibility of the possible damaged area.

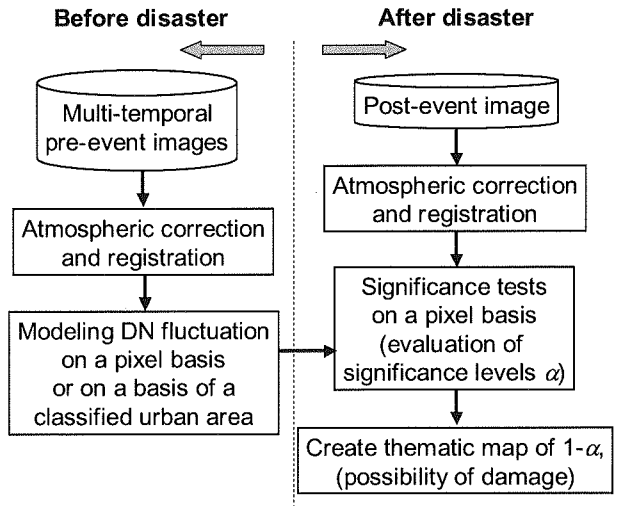

Figure 4. Flowchart of the Image Fluctuation Model method.

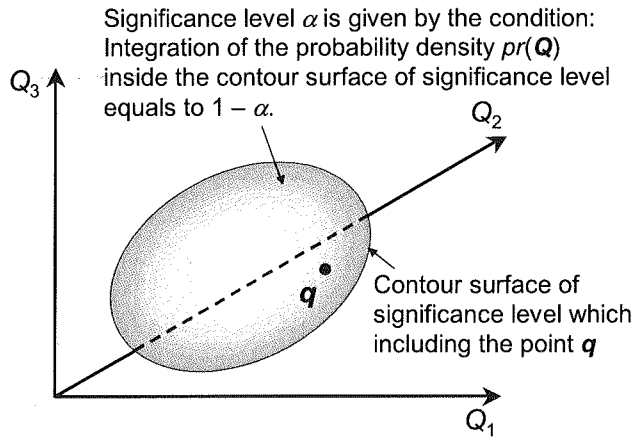

Figure 5. Determination of significance level α when the fluctuation model of digital numbers is expanded into a multidimensional probability distribution.

APPLICATION TO THE 2003 BAM, IRAN EARTHQUAKE

2003 Bam, Iran earthquake

The 2003 Bam, Iran earthquake occurred in the southeast of Iran and devastated Bam City in Kerman province. Eshghi and Zare (2003) reports that the Bam earthquake of December 26, 2003 (Mw6.5) occurred at 01:56:56 UTC (05:26:26 local time) around Bam City in the southeast of Iran. Since most of the residents were sleeping, the earthquake brought the great life loss: as of December 29, 2003, it was officially declared that the number of victims was more than 25,000, more than 50,000 people were injured, and about 100,000 people remained homeless; the population of Bam was about 100,000 at the time of the earthquake.

According to UN Office for the Coordination of Humanitarian Affairs (UN OCHA, 2004) as of March 17, 2004, the updated assessment of the impact of the earthquake, as provided by the Government of Iran, indicates that there are approximately 43,200 people dead, 15,000 still under medical treatment, 2,000 orphans and up to 90,000 people displaced in addition to the destruction of 50,000 houses in Bam and the surrounding rural areas. The number of people affected by loss of economic activity and damage to property and infrastructure is up to 200,000.

EOS/ASTER images used in the study

For detection of Bam City damage due to this earthquake, satellite images acquired by Advanced Spaceborne Thermal Emission and Reflection Radiometer of Earth Observing System (EOS/ASTER), was employed, of which the ground sampling distance is 15 meters for the three nadir-looking bands and one backward looking band of the visible and near infrared (VNIR) radiometer. Table 1 shows the spectral bands and looking directions of VNIR radiometer of EOS/ASTER. In this case study, twelve pre-event images and one post image of the product Level 1B (radiance registered at sensor) were used, which have very few or no clouds, as listed in Table 2. Figures 6 and 7 show the pre-event image of March 23, 2003 and the post-event image of January 2, 2004, respectively. In these images, red, green and blue colors represent Bands 3, 2 and 1, respectively.

Table 1. Spectral bands and looking directions of VNIR radiometer of EOS/ASTER.

Band name	Spectral range (wavelength range)	Looking direction
Band 1	0.52 - 0.60 μm	Nadir
Band 2	0.63 - 0.69 μm	Nadir
Band 3	0.76 - 0.86 μm	Nadir
Sterescopic band*	0.76 - 0.86 μm	Backward

*: not used in the study.

Table 2. Acquisition dates of EOS/ASTER images of Bam City used in the study.

Period	Number of images	Acquisition date (year-month-day)
Pre-event	12	2000-07-15, 2001-05-15, 2001-06-09, 2001-07-11, 2001-07-27, 2001-11-16, 2002-03-08, 2003-02-07, 2003-02-23, 2003-05-05, 2003-08-09, 2003-10-28
Post-event	1	2004-01-02

Modeling of digital number fluctuation

First, image registration was conducted with respect to the twelve pre-event images. Five ground control points (GCPs) surrounding Bam City were initially selected by visual interpretation. The locations of GCPs were sought with accuracy up to a fifth of pixel size (i.e. 3 m) so that the locations give the maximum image correlation with the master image of February 23, 2003 with respect to Band

2, which is expected to be relatively robust to vegetation change influence. In evaluation of image correlation, a window with size of 201×201 was used and a histogram of DNs in a window of an image to be registered (a slave image) is matched to that of the master image. Based on five pairs of the identified GCPs, the eleven slave images were registered by using warping method of rotation, scaling and translation and interpolation method of cubic convolution.

Then the mean and unbiased standard deviation of DNs were calculated pixel by pixel. By introducing assumption that the DN fluctuation can be modeled by a Gaussian distribution, these statistic parameters were used to construct a stochastic model of the DN fluctuation on a pixel basis. Figures 8 and 9 show the average and standard deviation images of the twelve pre-event, respectively.

Damage detection and discussions

Based on the derived stochastic models of DN fluctuation, the risk ratios were evaluated for the post-event image based on the DN fluctuation models of Gaussian distributions. Figure 10 shows the risk ratio distribution in the post event image with respect to Band 2. Figure 11 shows the risk ratio distribution in the pre-event image of October 28, 2003 with respect to Band 2. Note that, in the latter case, stochastic models were evaluated by using not twelve but eleven pre-event images acquired before October 28, 2003. The number of pixels with high risk ratio in Figure 11 is considerably smaller than in Figure 10. Hence, this fact supports that the proposed method may yield few commission errors (detection of false damage in non-damaged areas).

National Cartographic Center of Iran (2004) assessed the earthquake damage of Bam City based on aerial photographs and created a damage distribution map as a preliminary result. The map illustrates extensive damage in the east area of the city, which is nearer to the fault of the earthquake. In Figure 10, pixels with high risk ratios can be considered as the possible damaged areas. Pixels with high risk ratio appears more in the eastern part of the city and this has accordance with the result of National Cartographic Center of Iran (2004).

However, Space Imaging, Inc. (2004) depicts devastating damage in the entire residential area in Bam City with one-meter-resolution IKONOS image of December 27, 2003. Compared with this image, the damaged areas detected by the proposed method are clearly narrower than actual damage. Based on the visual inspection of a high resolution image of IKONOS, it is noticed that most of the buildings in the residential area reflect very similar spectrum and intensity even after their collapse or severe damage. Thus, texture or object-based analysis using high resolution image, in which shapes of buildings are easily identified, is necessary for more accurate damage detection in this city.

APPLICATION TO THE 2001 BHUJ, INDIA EARTHQUAKE

2001 Bhuj, India earthquake

A devastating earthquake of magnitude Mw 7.7 struck the Kachchh District, Gujarat State, India, at 3:16 UTC (8:46 local time) on January 26, 2001. This earthquake is called by different names, such as the Bhuj earthquake, Kachchh earthquake, Gujarat earthquake, and West India earthquake. The damage of the earthquake was the worst in India's recorded history. Extent of human loss was enormous with over 20,000 casualties, 166,000 people injured. Fully destroyed dwellings reached 370,000 units, and partially destroyed dwellings 920,000, and 600,000 people left homeless. The entire Kachchh region of Gujarat was extensively damaged, and several towns and large villages, like Bhuj, Anjaar, Vondh and Bhachau, sustained widespread destruction (Sato, et al., 2001; EERI, 2002).

EOS/ASTER images used in the study and modeling of digital number fluctuation

The EOS/ASTER VNIR images listed in Table 3 are employed to detect damage of Bhuj. In this study, only two pre-event images were available which cover Bhuj and include very few or little clouds. Due to this restriction, the following assumptions on a stochastic model of DN fluctuation is introduced:

a) The stochastic model of DN fluctuation is regarded as a Gaussian distribution.
b) The mean of the Gaussian distribution is given by the average DN of two pre-event images
c) All the pixel of urban structures subject to the stochastic models with the same standard deviation.

By the assumption c), the standard deviation was calculated by the root mean square of differences of DNs of two pre-event images. Figures 12 and 13 shows the pre-event image of October 11, 2000 and the post-event image of February 9, 2001, respectively.

Table 3. Acquisition dates of EOS/ASTER images of Bhuj used in the study.

Period	Number of images	Acquisition date (year-month-day)
Pre-event	2	2000-10-11, 2000-11-21
Post-event	1	2001-02-09

In the image registration, one GCP was used and the optimal location of the GCP was searched with accuracy up to a fifth of pixel size (i.e. 3 m) so that the location gives the maximum image correlation with the master image of October 11, 2000 with respect to Band 2. In evaluation of image correlation, a window with size of 2001×1201 was used and a histogram of DNs in a slave image is matched to that of the master image. Note that vegetation areas were excluded in histogram matching. Based on the identified GCP, the slave images were registered by translation and cubic convolution interpolation.

Then the mean image is derived from two pre-event images and the common standard deviation of Gaussian distributions was calculated from subtraction results of two DNs of pre-event images.

Damage detection and discussions

Based on the above stochastic models of DN fluctuation, the risk ratios were evaluated on a pixel basis for the post-event image. Figure 14 shows the risk ratio distribution in the post event image. In Figure 14, the maximum of three risk ratios of Bands 1, 2 and 3 is depicted on a pixel basis.

Chiroiu et al. (2002) assessed earthquake damage in Bhuj based on visual inspection of high-resolution satellite images of IKONOS and KVR-1000 as shown in Figure 15. The IKONOS image was taken two days after the earthquake (January 28, 2001) and one-meter-resolution pan-sharpened image (a combination of 1 meter panchromatic and 4 meters multispectral) was employed. Regarding a pre-event image, two-meter-resolution panchromatic KVR image acquired in 1998 was used. Because of the higher imaging capability, the damage detection result of Chiroiu et al. (2002) is considered to be so reliable that it can be used as a ground truth in verifying our damage detection result using EOS/ASTER images.

Comparing the two damage detection results, the followings can be pointed out:

- IFM method can detect areas including collapsed buildings and widely spread debris.
- Though area of damage detected by IFM method is slightly smaller than that of Chiroiu et al. (2002), the two damage detection results match mostly.

With respect to IFM method, the possible damage areas, which have high risk ratios, detected by using imagery of Band 3 (near infrared) is the largest in area. However, this may include influence of vegetation because this band is the most sensitive to the vegetation existence among the three bands of VNIR radiometer of EOS/ASTER. From the viewpoint of vegetation influence, Band 2 may be the most reliable among the three.

Some evacuee tents were detected as regions with high possibility of ground surface changes. It is, however, very difficult to distinguish these areas from truly damaged areas because the ground surface was really changed. It should be noted that this problem is due to the bounded imaging capability of a middle resolution sensor.

Figure 6. Pre-event image of Bam City acquired on February 23, 2003 (pseudo color).

Figure 7. Post-event image of Bam City acquired on January 2, 2004 (pseudo color).

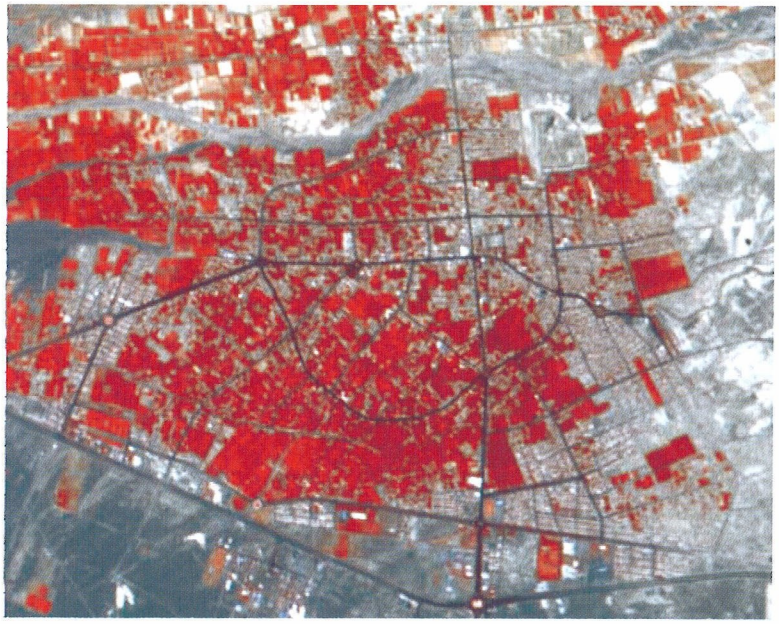

Figure 8. Average of the twelve pre-event images of Bam City (pseudo color).

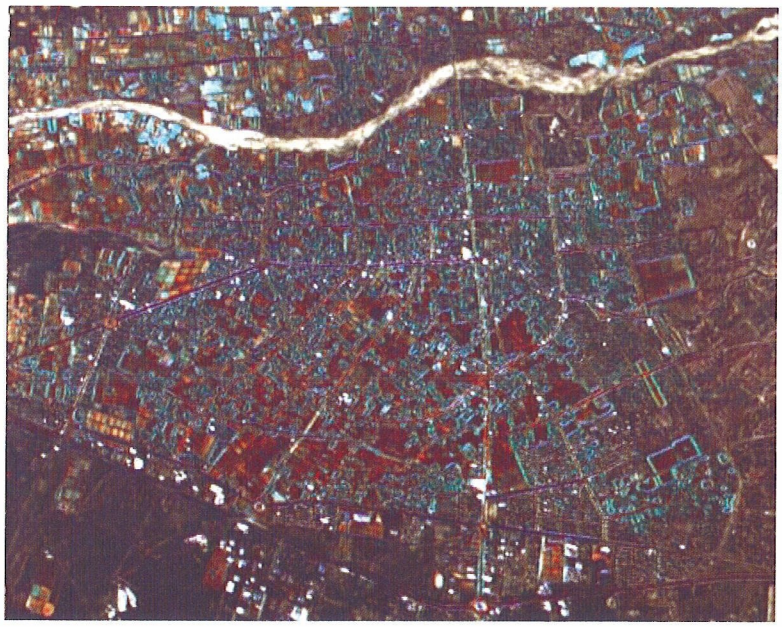

Figure 9. Standard deviation of the twelve pre-event images of Bam City (pseudo color).

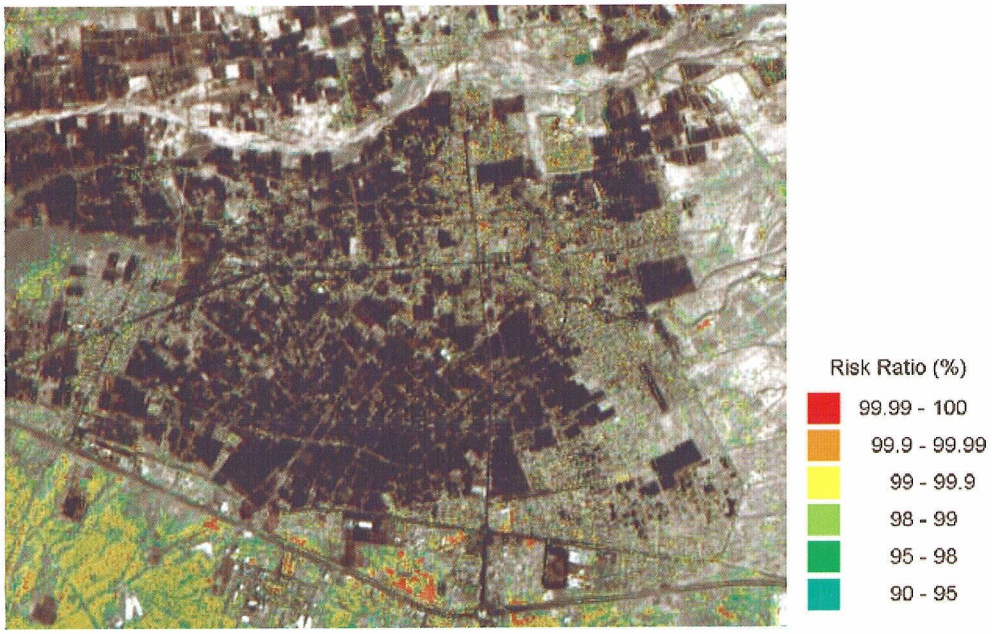

Figure 10. Risk ratio distribution of the post-event image of Bam City acquired on January 2, 2004.

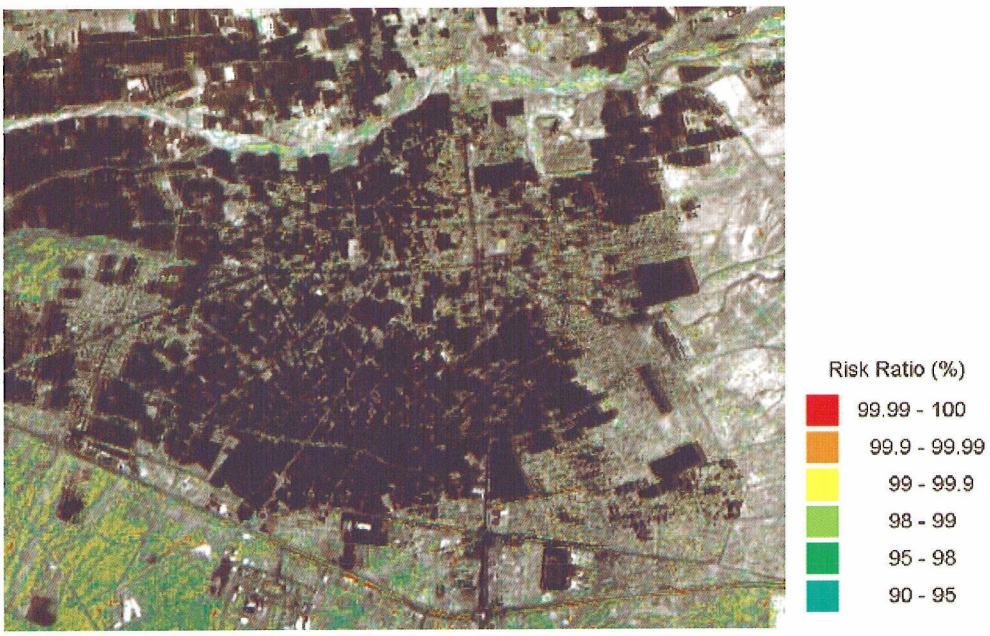

Figure 11. Risk ratio distribution of the pre-event image of Bam City acquired on October 28, 2003.

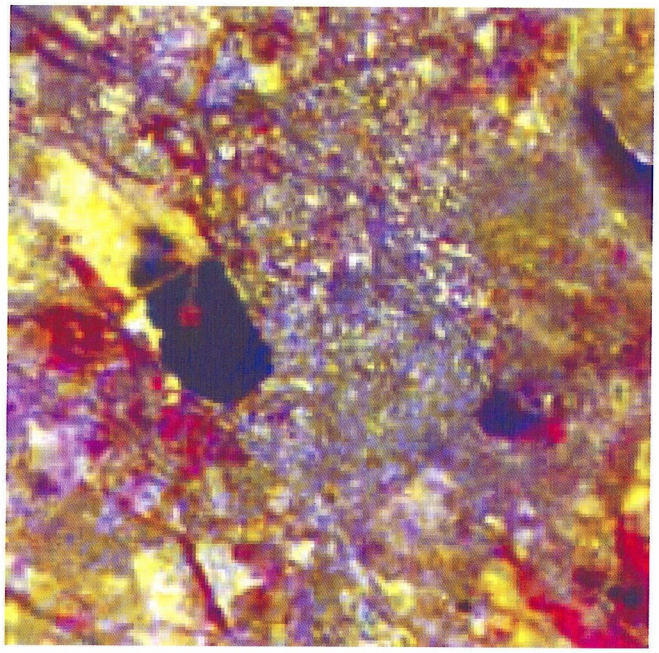

Figure 12. Pre-event image of Bhuj acquired on October 11, 2000 (pseudo color).

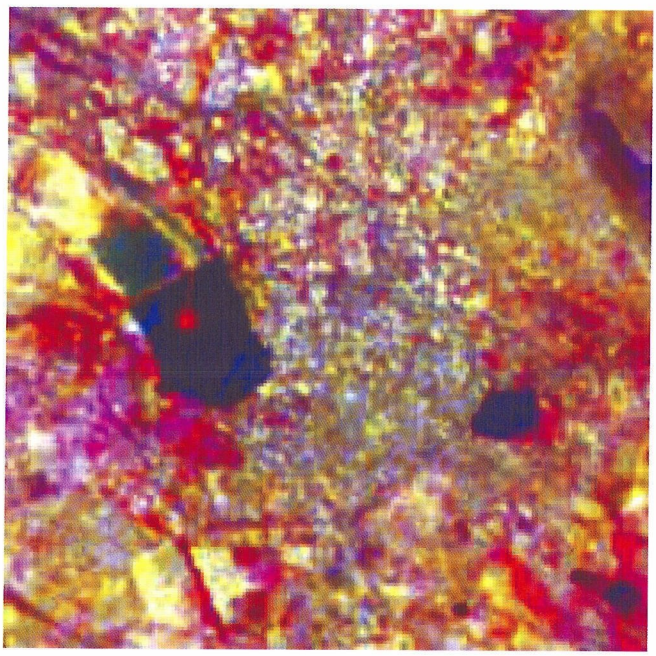

Figure 13. Post-event image of Bhuj acquired on February 9, 2001 (pseudo color).

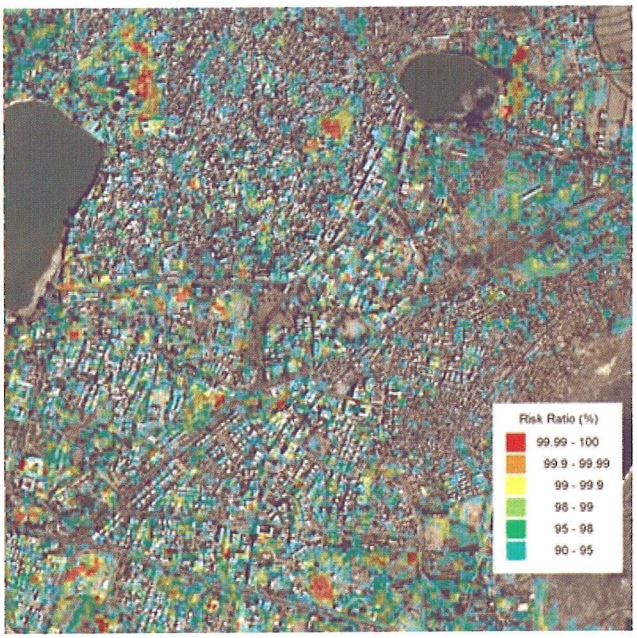

Figure 14. Risk ratio distribution of the post-event image of Bhuj acquired on February 9, 2001 overlaid on IKONOS pansharpened image.

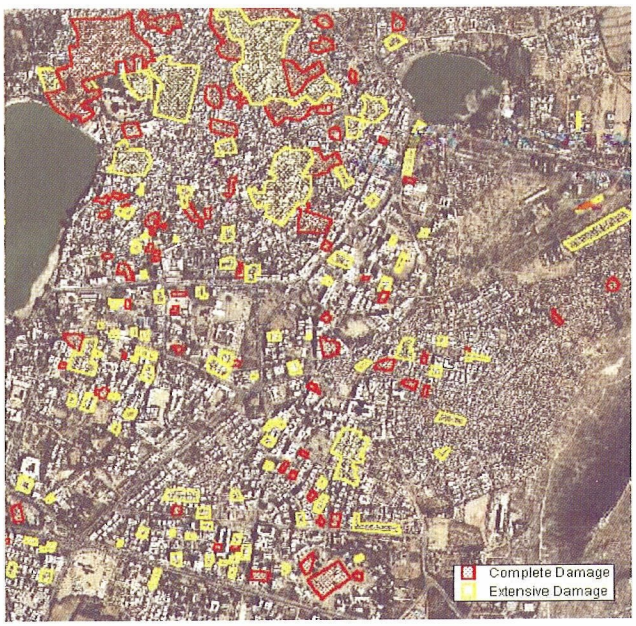

Figure 15. Damage of Bhuj assessed by Chiroiu et al. (2002) based on high-resolution satellite images.

CONCLUSIONS

A new damage (change) detection method, the image fluctuation model (IFM) method using middle-resolution satellite images, was proposed, which employs the probability distribution model of the DN fluctuation in a normal condition and its significance test. The resulting thematic map is created from the significance level to reject the null hypothesis that the pixel DN can be considered as a sample of the DN fluctuation model.

The proposed method was applied to two earthquakes, the 2001 Bhuj, India earthquake and the 2003 Bam, Iran earthquake using EOS/ASTER images. In the Bhuj earthquake case, twelve pre-event images were used to model DN fluctuation. In order to avoid vegetation influence, Band 2 images were used to create a risk ratio map of possible damaged areas. However, the detected damaged areas are narrower than the actual damaged areas observed by the high resolution satellite. This is because most of the buildings reflect very similar spectrum and intensity even after their collapse or severe damage. It was suggested that texture or object-based analysis using high resolution image is necessary for more accurate damage detection in this city.

In the Bam earthquake case, drastic assumptions were introduced in modeling of DN fluctuation because only two pre-event images were available. The maximum of three risk ratios of Bands 1, 2 and 3 was used to create a result map. The map was relatively similar to the visual inspection result of high resolution satellite images assessed by Chiroiu et al. (2002), however, some evacuee tents were detected as regions with high possibility of ground surface changes. It should be noted that recognition of this kind of small objects is very difficult for a middle resolution sensor due to the bounded imaging capability.

In future research, the validity of modeling and the accuracy of the IFM method should be examined based on other satellite images and further ground truth data of earthquake damage. In addition, DN fluctuation model of multi-band imagery using multi-dimensional Gaussian distribution should be examined for accuracy improvement.

ACKNOWLEDGMENTS

The EOS/ASTER data used in this study is owned by Ministry of Economy, Trade and Industry, Japan, and the data were provided by the ASTER announcement of research opportunities. The IKONOS images used in this study is owned by Space Imaging, Inc.

REFERENCES

Chiroiu, L., Andre, G., Guillande, R., and Bahoken, F. (2002). "Earthquake Damage Assessment Using High Resolution Satellite Imagery." *Proceedings of the 7th National Conference on Earthquake Engineering*, Earthquake Engineering Research Institute, CD-ROM, Paper#104, 10 pp., Boston, Massachusetts, U.S.A.

Dai, X. and Khorram, S. (1998). "The effects of image misregistraion on the accuracy of remotely sensed change detection." *IEEE Transactions on Geoscience and Remote Sensing,* Vol. 36, No. 5, 1566-1577.

Earthquake Engineering Research Institute (2002). "Bhuj, India, Earthquake of January 26, 2001, Reconnaissance Report", *Earthquake Spectra*, Supplement A to Vol. 18, 398 pp.

Eshghi, S and Zare, M. (2003). "Bam (SE Iran) earthquake of 26 December 2003, Mw6.5: A Preliminary Reconnaissance Report." http://www.iiees.ac.ir/English/bam_report_english_recc.html, as of December 29, 2003.

Kohiyama, M., Hayashi, H., Maki, N., Higashida, M, Kroehl, H.W., Elvidge, C.D., and Hobson V.R. (2004). "Early damaged area estimation system using DMSP/OLS night-time imagery." *International Journal of Remote Sensing* (in press).

Morisette, J.T., Khorram, S., and Mace, T. (1999). "Land-cover change detection enhanced with

generalized linear models." *International Journal of Remote Sensing*, Vol. 20, No. 14, 2703-2721.
National Cartographic Center of Iran (2004). "Earthquake Damage Map of Bam." http://www.ngdir.ir/Downloads/Downloads.asp, as of March 23, 2004.
Sato, T. et al. (2001). *A comprehensive survey of the 26 January 2001 earthquake (Mw7.7) in the State of Gujarat, India*. Report by the research team supported by the grant-in-aid for specially promoted research provided by the Japanese Ministry of Education, Culture, Sports, Science and Technology in the fiscal year of 2000, Grant No. 12800019, Japan.
Schowengerdt R.A. (1997). *Remote Sensing: Models and Methods for Image Processing*, Second Edition, Academic Press, San Diego, USA.
Singh, A. (1989). "Digital change detection techniques using remotely-sensed data." *International Journal of Remote Sensing,* Vol. 10, No. 6, 989-1003.
Space Imaging, Inc. (2004) "Zoom Gallery: Bam, Iran." Zoom Gallery Archive, Earthquake damage in Bam, Iran. http://www.spaceimaging.com/gallery/zoomify/bam.htm, as of March 23, 2004
UN Office for the Coordination of Humanitarian Affairs (2004). "Iran - Earthquake OCHA Situation Report No. 15." http://www.reliefweb.int, as of March 17, 2004.